

## Cross section for the primordial reaction ${}^8\text{Li}(p, n){}^8\text{Be}(\text{g.s.})$ at $E_{\text{c.m.}}=1.5$ MeV

D. D. Caussyn,\* N. R. Fletcher, K. W. Kemper, and E. E. Towers  
*Department of Physics, Florida State University, Tallahassee, Florida 32306*

J. J. Kolata, K. Lamkin, and R. J. Smith†  
*Department of Physics, University of Notre Dame, Notre Dame, Indiana 46556*

F. D. Becchetti, J. A. Brown, J. W. Jänecke, and D. A. Roberts  
*Department of Physics, University of Michigan, Ann Arbor, Michigan 48109*

D. L. Gay  
*Department of Natural Sciences, University of North Florida, Jacksonville, Florida 32216*  
(Received 27 August 1992)

The differential cross section for the primordial reaction  ${}^8\text{Li}(p, n){}^8\text{Be}(\text{g.s.})$  has been determined at  $E_{\text{c.m.}} = 1.5$  MeV in the c.m. angular range  $38^\circ$  to  $90^\circ$  by use of the radioactive nuclear beam facility at the University of Notre Dame which utilizes a superconducting solenoid lens system designed at the University of Michigan, and a  ${}^8\text{Be}$  detection technique developed at the Florida State University. A  ${}^8\text{Li}$  beam of approximately  $10^7$  pps is used to infer a total cross section of  $21 \pm 2$  mb, with a 20% absolute cross section uncertainty. This total cross section is a factor of two smaller than a conventional Hauser-Feshbach calculation and it is also much smaller than that of some other  ${}^8\text{Li}$  burning reactions.

PACS number(s): 25.40.-h, 97.10.Cv

For the past several years there has been an intensifying interest in the production and use of radioactive nuclear beams (RNB) for the study of exotic nuclear reactions. An important application of cross section measurements resulting from RNB is in tests of models of primordial nucleosynthesis of light nuclides [1]. Since an important avenue to heavier elements in the inhomogeneous models of primordial nucleosynthesis [2] is  ${}^{11}\text{B}$  production, primarily in the reaction  ${}^8\text{Li}(\alpha, n){}^{11}\text{B}$ , it is important to investigate all modes of  ${}^8\text{Li}$  burning. In these models the low density regions are characterized by a neutron excess and a corresponding excess of neutron rich isotopes such as  ${}^8\text{Li}$ , and the high density regions are characterized by proton excesses. One would therefore expect the  ${}^8\text{Li}(p, n){}^8\text{Be}$  reaction to be of importance only in regions near the density boundaries, except when abundances are rapidly changing during the homogenization phase [3].

Measurement of the  ${}^8\text{Li}(p, n){}^8\text{Be}(\text{g.s.})$  cross section provides us with some rather unique challenges. Not only is the residual nucleus,  ${}^8\text{Be}(\text{g.s.})$ , unstable ( $t_{1/2} \simeq 6 \times$

$10^{-16}$  sec) but the detection of the neutron yield from the reaction is impossibly bathed in an intense neutron background from the breakup of the  ${}^8\text{Li}$  beam used in the currently measured inverse reaction,  $p({}^8\text{Li}, {}^8\text{Be})n$ , and from other reactions occurring along with the  ${}^8\text{Li}$  production reaction. In spite of these problems, the measurement of the  $p({}^8\text{Li}, {}^8\text{Be})n$  reaction can be accomplished since the  ${}^8\text{Li}$  beam at the University of Notre Dame RNB facility is one of the purest low-energy radioactive beams and the identification of  ${}^8\text{Be}(\text{g.s.})$  is quite unique in our detection method.

The University of Notre Dame (UND) radioactive beam facility at the UND FN-Tandem laboratory can provide  ${}^8\text{Li}$  beam particles at a rate of  $\sim 10^7$  pps by bombarding a  ${}^9\text{Be}$  primary target of areal density  $\sim 2.3$  mg/cm<sup>2</sup> with 17 MeV  ${}^7\text{Li}$  ions from the FN-Tandem accelerator [4]. The  ${}^8\text{Li}$  particles produced in the  ${}^9\text{Be}({}^7\text{Li}, {}^8\text{Li}){}^8\text{Be}$  reaction are focused onto a secondary target by use of a superconducting solenoid [5] equipped with an axial beam stop, such that it accepts reaction products in the laboratory angular range of  $5^\circ$  to  $11^\circ$ . At the appropriate magnetic field setting the  ${}^8\text{Li}$  particles form a beam spot with diameter of approximately 5 mm and with an angular divergence of  $\pm 3^\circ$ . A secondary target of  $\text{CH}_2$  was used to study the reaction of interest and a natural carbon target was used to determine the background.

The  ${}^8\text{Be}$  detector consists of two 1 cm  $\times$  5 cm  $\times$  3000  $\mu\text{m}$  thick, position-sensitive, silicon detectors operated in coincidence. They are mounted symmetrically above

\*Current address: Indiana University Cyclotron Facility, Bloomington, Indiana 47405.

†Current address: Division of Nuclear Medicine, Department of Radiology, University of Pennsylvania Hospital, Philadelphia, PA 19104.

and below the horizontal reaction plane, with their 5 cm position-sensitive directions parallel and separated by 3.6 mm. The pair is located approximately 10 cm from the secondary target. Prior to an experiment each detector segment is calibrated in energy and position by use of a  $^{228}\text{Th}$  radioactive source which gives six well-defined alpha-particle energies between 5.3 and 8.8 MeV. A grid of 21 vertical slit apertures, of known width and separation in a 0.5 mm thick Ta mask, is placed in front of each detector segment for the position calibration. Position and energy resolutions for alpha-particle detection are typically 0.7 mm and 100 keV [full width at half maximum (FWHM)], respectively. The interdependence of energy and position in the calibration, the energy-dependent efficiency for  $^8\text{Be}$  detection, and the decay kinematics for calculating the relative energy between the decay alpha particles and thereby uniquely identifying the  $^8\text{Be}(g.s.)$ , all have been discussed in great detail elsewhere [6].

The  $^8\text{Be}(g.s.)$  production rate in the reaction  $p(^8\text{Li}, ^8\text{Be})n$  is expected and observed to be very low, partly because of the limited intensity of the secondary beam of  $^8\text{Li}$  particles. Consequently, we found it advantageous to calibrate by use of the prolific yield from the  $^{12}\text{C}(^7\text{Li}, ^8\text{Be})^{11}\text{B}$  reaction. This was conveniently done with a relatively intense secondary beam of  $^7\text{Li}$  ions by reducing the solenoid field such as to focus  $^7\text{Li}$  ions elastically scattered from the primary  $^9\text{Be}$  target onto the secondary target. The  $^7\text{Li}$ -induced reaction allowed us to verify the unambiguous identification of detected  $^8\text{Be}$  particles, and also to establish corrections for beam angle and beam energy for the relatively poorly defined secondary  $^8\text{Li}$  beam.

Accurate values of the secondary beam energy and angle were determined through the use of three-body final state kinematics. In these reactions, two of the final state particles are the alpha particles whose energies and positions are measured in the  $^8\text{Be}$  detector. With these vector momenta determined, the third particle momentum is calculated event by event, and then the three-body  $Q$ -value spectrum can be calculated [6]. This measured  $Q$ -value spectrum for the  $^{12}\text{C}(^7\text{Li}, ^8\text{Be}(g.s.))$  reactions, which is shown in Fig. 1, is the result of a run time of approximately 30 minutes on a carbon target of areal density  $940 \mu\text{g}/\text{cm}^2$ . The data of Fig. 1 represent an angular range of detected  $^8\text{Be}$  events of approximately  $10^\circ$  to  $33^\circ$  in the laboratory. The nominal angle of the detector center is adjusted, in the data reduction, until the calculated  $Q$ -values are independent of reaction angle. This procedure results in a correction to the nominal angle setting of  $-1.6^\circ$ . Similarly, in the data reduction, the secondary beam energy is adjusted until the events in a two-dimensional scatter plot of  $^8\text{Be}$  energy vs  $^8\text{Be}$  reaction angle follow the calculated two-body kinematics result. This procedure resulted in a correction to the nominal beam energy of  $-100$  keV to the final value of  $14.2$  MeV. These corrections are small, but the angular correction in particular is very important for the  $p(^8\text{Li}, ^8\text{Be})n$  reaction where the inverse two-body kinematic effects are extreme.

The  $^8\text{Be}(g.s.)$  events are initially identified in a two-

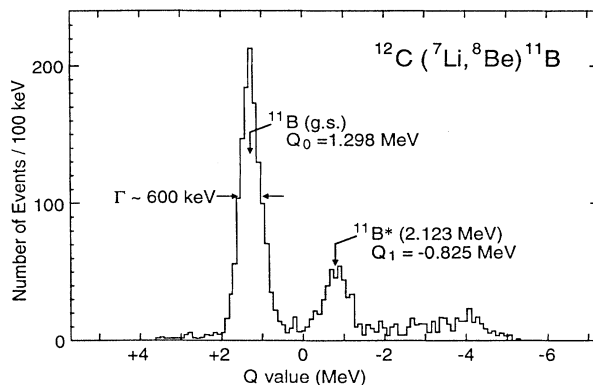


FIG. 1.  $Q$ -value spectrum for the reaction  $^{12}\text{C}(^7\text{Li}, ^8\text{Be}(g.s.))^{11}\text{B}$ , using a secondary beam of  $^7\text{Li}$  particles.

dimensional plot of the energies of the two alpha particles detected in coincidence. The identification is confirmed by calculating [6] the relative energy between the two alpha particles for each selected coincidence event. A relative energy spectrum for the events in the ground-state  $Q$ -value peak of Fig. 1 is shown in Fig. 2(a). The measured decay energy is observed to be very close to the known value of 92 keV. The relative energy spectra of Fig. 2 demonstrate clearly that there is no significant contribution to our final cross section values from excited  $^8\text{Be}$  events, since those events would produce relative energies of 1 to 5 MeV. The small corrections to reaction angle and bombarding energy, discussed above, have already been made for the data shown in both Figs. 1 and 2. The observed energy resolution in Fig. 1 is primarily the net effect of beam divergence, spot size, and energy spreading due to the effects of target thickness and the finite angular opening of the solenoid. The energy resolution in Fig. 2 is dependent primarily on detector position and energy resolutions and the fact that we measure only the in-plane momenta of the alpha particles, but

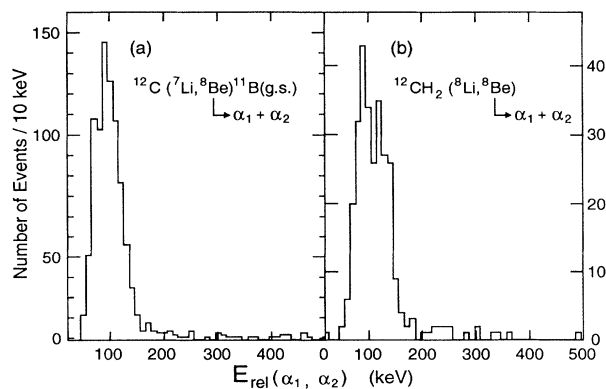


FIG. 2. Relative energy between the coincidence detected alpha particles identified as  $^8\text{Be}$  events. The  $^8\text{Be}(g.s.)$  decay energy is 92 keV. Since only the in-plane separation of alpha particles is measured, the larger energy range of detected  $^8\text{Be}$  particles in case (b) increases the energy spread with which the  $^8\text{Be}$  decay energy is identified.

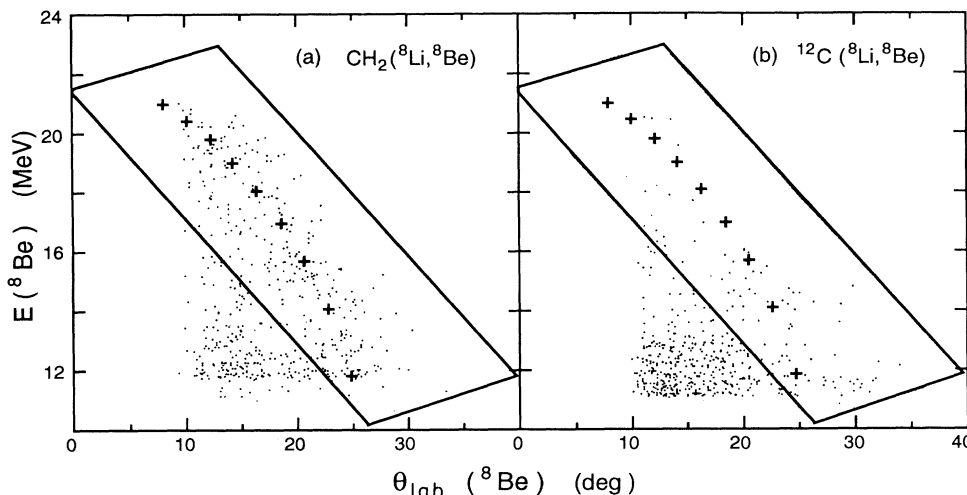


FIG. 3. Scatter plot of  ${}^8\text{Be}$  energy versus laboratory reaction angle. Events within the parallelogram are accepted for (a) the reaction of interest, and for (b) determining background. The crosses indicate the kinematic calculations for the  $p({}^8\text{Li}, {}^8\text{Be}(\text{g.s.}))n$  reaction.

it is nearly independent of all other resolution-degrading effects including the parameters of the  ${}^8\text{Li}$  beam.

The data for the  $p({}^8\text{Li}, {}^8\text{Be})n$  experiment were gathered from a 39 h  ${}^8\text{Li}$  bombardment of a  $\text{CH}_2$  target having areal density  $720 \mu\text{g}/\text{cm}^2$ . Identification of the reaction of interest by forming a  $Q$ -value spectrum as was done for the  ${}^{12}\text{C}({}^7\text{Li}, {}^8\text{Be}){}^{11}\text{B}$  reaction, Fig. 1, is not possible, since kinematic effects produce an energy resolution of  $\sim 3$  MeV and the events from the carbon content in the target form a nonseparated background. The detection of  ${}^8\text{Be}(\text{g.s.})$  events is still clearly identified [as seen in Fig. 2(b)], and as long as we are dealing with high positive  $Q$ -value reactions they are separated from the bothersome continuum caused by a very intense neutron-induced background. The separation of  ${}^8\text{Be}$  events from the proton and carbon components of the target is accomplished simply by forming the scatter plot of  ${}^8\text{Be}$  energy versus the calculated laboratory reaction angle, drawing a liberal two-dimensional gate around the appropriate kinematic region, which also shows a clear preponderance of events, and subtracting the appropriately normalized number of events within the same gate from a 45 h bombardment of the  $940 \mu\text{g}/\text{cm}^2$  carbon target (see Fig. 3). The total number of events within the gate was 254 for the  $\text{CH}_2$  target and 83 for the carbon target. The spectrum of relative energy between alpha particles for the gated events of Fig. 3(a) is shown in Fig. 2(b), again clearly identifying the events as  ${}^8\text{Be}(\text{g.s.})$  particles. The background-subtracted data are binned in  $3^\circ$  segments in laboratory angle, the approximate angular resolution of the incident secondary beam. The yields are then converted to differential cross sections. The absolute cross section was determined by use of  ${}^8\text{Li}$  Rutherford scattering from a Au target and employing a monitor detector in the production chamber to normalize the rate of incident  ${}^8\text{Li}$  particles. The final cross section results for  ${}^8\text{Be}(\text{g.s.})$  formation are shown in Fig. 4.

A cross section determination for formation of  ${}^8\text{Be}(J^\pi=2^+)$  would be highly desirable and it is expected

to be greater than for  ${}^8\text{Be}(\text{g.s.})$  formation. The spectrum of Fig. 2(b) is not expected to show  ${}^8\text{Be}(2^+)$  events since it is generated for events within the kinematic gate of Fig. 3(a). Events of  ${}^8\text{Be}(2^+)$  production would appear approximately 3 MeV below the kinematic line for the ground state events in Fig. 3 and their kinetic energy would be spread well into the background of events from the carbon component of the target. The extreme kinematic effects coupled with the angular range of the detector, its very small efficiency for  ${}^8\text{Be}(2^+)$  detection and its lack of vertical position information, the broad width of the first excited state of  ${}^8\text{Be}$ , and the background contributions from the carbon component of the target and neutron events in the detectors, make both the identification and the simulation of  ${}^8\text{Be}(2^+)$  events extremely unreliable for the current detector geometry.

Measurements [7] of the  ${}^7\text{Li}(p, n){}^7\text{Be}(\text{g.s.})$  reaction in roughly the same energy region show this cross section to be 10 times larger than that for the  ${}^8\text{Li}(p, n){}^8\text{Be}(\text{g.s.})$  reaction. In addition, the  ${}^7\text{Li}(p, n){}^7\text{Be}(\text{g.s.})$  angu-

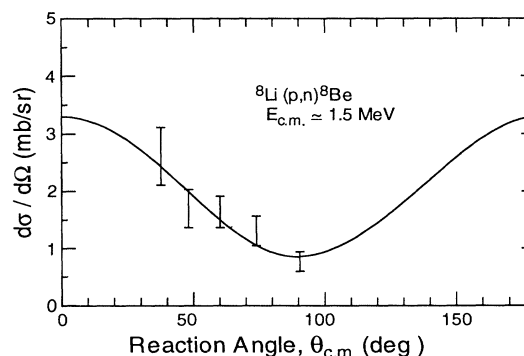


FIG. 4. Differential cross section for the reaction  ${}^8\text{Li}(p, n){}^8\text{Be}(\text{g.s.})$ . Error bars are statistical only. The curve represents a fit by the function  $A_0 + A_2P_2(\cos\theta)$ , with  $4\pi A_0 = 21 \pm 2$  mb and  $A_2/A_0 \approx 0.9 \pm 0.4$ .

TABLE I. Optical model parameters used in Hauser-Feshbach calculations.

Particle pair	$U$ (MeV)	$R_R$ (fm)	$a_R$ (fm)	$W$ (MeV)	$R_I$ (fm)	$a_I$ (fm)
${}^8\text{Li} + p$	46.05	2.50	0.65	6.00	2.50	0.47
${}^8\text{Be} + n$	41.24	2.63	0.66	8.51	2.53	0.48
${}^5\text{He} + {}^4\text{He}$	196.60	3.39	0.48	9.2	3.39	0.48
${}^7\text{Li} + {}^2\text{H}$	78.00	2.01	0.95	30.00	1.61	0.85
${}^6\text{Li} + {}^3\text{H}$	145.00	1.54	0.70	1.91	3.74	0.72
${}^8\text{Li} + p^a$	46.45	2.37	0.48	6.34	2.37	0.72
${}^8\text{Be} + n^b$	40.67	2.80	0.62	22.20	2.80	0.90

<sup>a</sup>Alternate parameter set from Ref. [15].

<sup>b</sup>Alternate parameter set from Ref. [16].

lar distributions are symmetric about  $90^\circ$  c.m., for energies not dominated by resonances, suggesting that this reaction proceeds by the compound nucleus mechanism at these low proton energies. To determine if the  ${}^8\text{Li}(p,n){}^8\text{Be}(\text{g.s.})$  reaction is also dominated by the compound-nucleus mechanism, Hauser-Feshbach (HF) cross sections [8] were generated by use of the computer program HELGA [9]. The calculations include decay channels leading to five residual pairs. For  ${}^8\text{Li}+p$  interactions at center-of-mass energies less than 2 MeV, the maximum energies available to excite the residuals are sufficiently small that all possible decays are to discrete levels. If there exist extra unknown discrete levels, then this HF calculation is an overestimate. Excitation energies, spins, and parities of residual states were taken from standard compilations [10]. Table I shows the optical-model parameters from which transmission coefficients were determined. Since optical potentials determined from elastic scattering experiments are not available for several of the residual pairs, there is some latitude in the choice of parameter sets. Systematic potentials were used for the proton [11] and neutron [12] channels. Parameter sets for  ${}^6\text{Li} + \alpha$  [13] and  ${}^9\text{Be} + t$  [14] were employed for the  ${}^5\text{He} + \alpha$  and  ${}^6\text{Li}+t$  channels, respectively. This calculation produces a HF total cross section of about 46 mb. The sensitivity of the calculation to the parameters was checked by using several alternate parameter sets. It was most sensitive to the parameters for the proton and neutron channels, where the alternate parameter sets listed

in Table I produced increases in the integrated cross section of up to 20%.

The experimental total cross section can be approximated by assuming a functional form for the angular distribution which is consistent with the Hauser-Feshbach calculation, i.e.,  $\sigma(\theta) = A_0 + A_2P_2(\cos\theta)$ . The parameters of the curve shown in Fig. 4 yield  $\sigma_T = 4\pi A_0 = 21 \pm 2$  mb where the uncertainty is based on statistical errors in the data only. The absolute uncertainty in the total cross section is the order of 20%. Obviously it is questionable to apply the HF technique at such low energies. The measured value is a factor of 2 less than the HF calculation. It is also much less than that for the recently measured  ${}^8\text{Li}(p,\alpha){}^5\text{He}$  reaction [17]. From the gates of Fig. 3 one can argue that we have missed some  ${}^8\text{Be}$  events at the maximum angles ( $\theta_{\text{c.m.}} \sim 90^\circ$ , Fig. 4), but even by eliminating this data point, the experimental value of  $\sigma_T$  is increased by only  $\sim 10\%$  while  $A_2/A_0$  is decreased by 20%. One can then infer that at astrophysical energies ( $<300$  keV) the already very small cross section would be quite insignificant in the absence of strong resonant effects. We conclude that the  ${}^8\text{Li}(p,n){}^8\text{Be}(\text{g.s.})$  reaction is not a dominant  ${}^8\text{Li}$  burning reaction in astrophysical models for nucleosynthesis.

This work was supported in part by the National Science Foundation, Grant Nos. PHY-8900689 (FSU), PHY-9100708 (UND), and PHY-891131 (UM).

- 
- [1] W.A. Fowler, Rev. Mod. Phys. **56**, 149 (1984); *Proceedings of the Workshop on Prospects for Research with Radioactive Beams from Heavy Ion Accelerators*, edited by J.M. Nitschke (Lawrence Berkeley Laboratory Report No. LBL-18187, 1984); "Research Opportunities with Radioactive Nuclear Beams," The Isospin Laboratory LALP Report No. 91-95, 1991.
- [2] J.H. Applegate, C.J. Hogan, and R.J. Scherrer, *Astrophys. J.* **329**, 592 (1988); C. Alcock, G.M. Fuller, and G.J. Mathews, *Astrophys. J.* **320**, 439 (1987); R.A. Malaney and W.A. Fowler, *Astrophys. J.* **333**, 14 (1989); T. Kajino and R.N. Boyd, *Astrophys. J.* **359**, 267 (1990).
- [3] R.N. Boyd (private communication).
- [4] F.D. Becchetti, J.A. Brown, K. Ashktorab, J.W. Jänecke, W.Z. Liu, D.A. Roberts, R.J. Smith, J.J. Kolata, K. Lamkin, A. Morsad, and R.E. Warner, *Nucl. Instrum. Methods Phys. Res. Sect. B* **56/57**, 554 (1991).
- [5] R.L. Stern, F.D. Becchetti, T. Casey, J.W. Jänecke, P.M. Lister, W.Z. Liu, D.G. Kovar, R.V.F. Janssens, M.F. Vineyard, W.R. Phillips, and J.J. Kolata, *Rev. Sci. Instrum.* **58**, 1682 (1987).
- [6] D.D. Caussyn, G.L. Gentry, J.A. Liendo, N.R. Fletcher, and J.F. Mateja, *Phys. Rev. C* **43**, 205 (1991); Florida State University Superconducting Accelerator Laboratory Progress Report, 1986-88, pp. 70-85; D.D. Caussyn, Ph.D. thesis, Florida State University, 1990.

- [7] S.A. Elbakr, I.J. Van Heerden, W.J. McDonald, and G.C. Neilson, *Nucl. Instrum. Methods* **105**, 519 (1972).
- [8] E. Vogt, in *Advances in Nuclear Science*, edited by M. Baranger and E. Vogt (Plenum, New York, 1968), Vol. 1.
- [9] S.K. Penney (unpublished).
- [10] F. Ajzenberg-Selove, *Nucl. Phys.* **A490**, 1 (1988); C.M. Lederer and V.S. Shirley, *Table of Isotopes*, 7th ed. (Wiley-Interscience, New York, 1978).
- [11] F.G. Perey as listed in P.E. Hodgson, *Nuclear Reactions and Nuclear Structure* (Clarendon, Oxford, 1971), p. 175.
- [12] D. Wilmore and P.E. Hodgson as listed in P.E. Hodgson, *Nuclear Reactions and Nuclear Structure* (Clarendon, Oxford, 1971), p. 174.
- [13] H.G. Bingham, K.W. Kemper, and N.R. Fletcher, *Nucl. Phys.* **A175**, 374 (1971).
- [14] G.H. Herling, L. Cohen, and J.D. Silverstein, *Phys. Rev.* **178**, 1551 (1969), as listed in C.M. Perey and F.G. Perey, *Atomic Data and Nuclear Data Tables* (Academic, New York, 1976), Vol. 17, p. 64.
- [15] L.A. Kull, as listed in C.M. Perey and F.G. Perey [14], p. 20.
- [16] H.F. Lutz, J.B. Mason, and M.D. Karvelis, as listed in *Atomic Data and Nuclear Data Tables* [14], p. 10.
- [17] F.D. Becchetti, J.A. Brown, W.Z. Liu, J.W. Jänecke, D.A. Roberts, J.J. Kolata, R.J. Smith, K. Lamkin, A. Morsad, R.E. Warner, R.N. Boyd, and J.D. Kalen, *Nucl. Phys. A* (to be published).